MICHIGAN STATE UNIVERSITY

CYCLOTRON LABORATORY

STUDY OF THE (p, ^{3}He) AND (p, t) REACTIONS ON ^{29}Si

H. NANN, W. BENENSON, W.A. LANFORD and B.H. WILDENTHAL

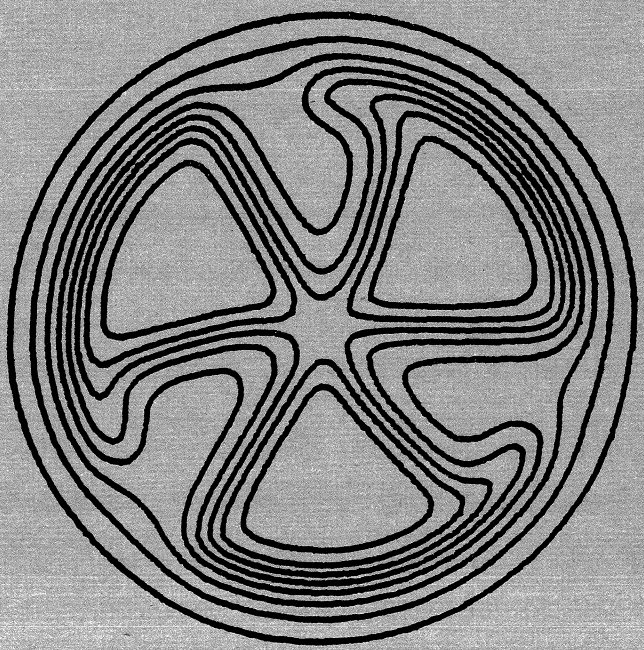

MSUCL-122 MAY 1974

Study of the $(p,^3He)$ and (p,t) Reactions on ^{29}Si[†]

H. Mann,[††] W. Benenson, W.A. Lanford[†††] and B.H. Wildenthal

Cyclotron Laboratory, Department of Physics
Michigan State University, East Lansing, Michigan 48824

ABSTRACT

Differential cross sections of the $^{29}Si(p,^3He)^{27}Al$ and $^{29}Si(p,t)^{27}Si$ reactions between θ_L=4° and 60° have been measured at 40.1 MeV bombarding energy. Assignments of the L-transfers on the basis of comparisons to DWBA calculations yield several new spin and parity assignments for states in ^{27}Si. The experimental differential cross sections of the transitions to several of the low-lying mirror pairs of final states in ^{27}Al and ^{27}Si are compared to the results of microscopic DWBA calculations in order to study the spin-isospin dependence of the interaction potential in the two-nucleon transfer reaction and to test current shell-model wave functions for the nuclear states involved.

[NUCLEAR REACTIONS: $^{29}Si(p,t)^{27}Si$, $^{29}Si(p,^3He)^{27}Al$, E_p=40.1 MeV; Measured $\sigma(E_t,E_{^3He},\theta)$; Enriched target; deduced energies, L-values, normalization factors for states of ^{27}Al and ^{27}Si.]

[†]Supported in part by the U.S. National Science Foundation.

[††]On leave of absence from Institut für Kernphysik der J.W. Goethe Universität, Frankfurt/M, Germany.

[†††]Now at Yale University, New Haven, Connecticut.

I. INTRODUCTION

The simultaneous investigation of $(p,^3He)$ and (p,t) reactions on T_z=½ targets leading to mirror states in the residual nuclei is of interest for two reasons. Firstly, since the wave functions of the mirror states are essentially identical, the effects of a spin and isospin dependent interaction potential in the distorted-wave Born approximation (DWBA) analysis of the two-nucleon transfer reactions[1] can be studied by comparing the $(p,^3He)$ and (p,t) cross sections. Secondly, since the $(p,^3He)$ reaction permits the transfer of a proton-neutron pair both in the singlet (S=0,T=1) and in the triplet (S=1,T=0) states, whereas the (p,t) reaction allows the transfer of two neutrons only in the singlet (S=0,T=1) state, it is possible to study in a comparative way different parts of the wave functions of the target and the residual nuclei. It is a complicating feature of the problem that these two aspects are coupled to each other. The accuracy of the determination of the characteristics of the spin-isospin term in the interaction potential depends upon the reliability of the wave functions used in the analysis and, conversely, a meaningful test of wave functions by means of a $(p,^3He)$-(p,t) comparison can only be carried out with an accurate knowledge of this same spin-isospin dependent part of the interaction potential used in the DWBA analysis.

Previous work[2-8] in the comparative study of $(p,^3He)$ and (p,t) reactions to mirror levels has been carried out principally

with 1p shell and, to a lesser extent, 2s-1d shell nuclei. These investigations have been handicapped generally by the lack of theoretical wave functions for the nuclear states involved. The present availability of rather thoroughly tested wave functions for 2s-1d shell nuclei[9-12] suggests that further work on this topic in this region might be rewarding. The present study of the (p,t) and (p,^{3}He) reactions on ^{29}Si is a part of a systematic investigation of the (^{3}He,p), (p,^{3}He) and (p,t) reactions on T_z=1/2 target nuclei in the 2s-1d shell.[13-16] The dual aims are, as mentioned, to arrive at the most secure conclusions possible about the spin-isospin dependence of the interaction potential by studying the widest feasible variety of experimental and theoretical examples and, in each individual case, to make whatever critique is possible about the model wave functions used in the analysis. In addition, the experimental data should yield some new spectroscopic assignments independent of the detailed theoretical analysis.

II. EXPERIMENTAL PROCEDURE

The experiment was performed with a 40.1 MeV proton beam from the Michigan State University Cyclotron. The target consisted of SiO and SiO_2, enriched to 95% in ^{29}Si, deposited by vacuum evaporation on a thin layer of formvar. The effective thickness of the Si+O layer was approximately 0.06 mg/cm^2. The reaction products were detected in a 30 cm long position-sensitive single-wire gas proportional counter placed in the focal plane

of a split-pole magnetic spectrograph.[17] The proportional counter was backed by a scintillation counter which was run in coincidence with it to provide background suppression and particle identification. An overall energy resolution of 25-30 keV was obtained with this system.

Fig. 1 shows spectra for ^{29}Si(p,t)^{27}Si (upper half) and ^{29}Si(p,^{3}He)^{27}Al (lower half) taken at $\theta_{Lab.}$=8°. States up to an excitation energy of 5.3 and 6.3 MeV, respectively, were observed, and are populated with reasonable intensity. The ground state intensities are about an order of magnitude larger than those of any of the excited states. Groups due to contaminants are cross hatched and labeled by the residual nucleus and the corresponding excitation energy. Unfortunately, at smaller angles some ^{3}He-particle groups from the ^{29}Si(p,^{3}He)^{27}Al reaction coincide with groups from the contaminant ^{28}Si(p,^{3}He)^{26}Al reaction, so that their angular distributions could not be taken.

The cross section normalization was established both by comparing the ^{29}Si(p,d)^{28}Si ground state cross section obtained with the enriched ^{29}Si targets to that from a thicker natural Si target the thickness of which was measured by the attenuation of alpha particle energies and by measuring the ratio of the (p,t) cross sections to the elastic scattering cross sections in the θ_L=25°-50° region. In this latter procedure the elastic scattering cross sections were assumed to have the average of the values calculated in the optical model from the parameters of Greenlees and Pyle and of Bechetti and Greenlees.[18] The accuracy

of the absolute differential cross sections is estimated to be about 20%, and an error of 10% is estimated for the relative (p,t) to (p,^{3}He) cross section scales.

The energy resolution with which the present data were acquired may be characterized in relative terms as good for (p,t) and excellent for (p,^{3}He). The suppression of background, chiefly deuterons for the (p,t) runs, and protons, deuterons and ^{4}He's for the (p,^{3}He) runs is likewise excellent. The 40 MeV incident energy should be sufficient to eliminate most non-direct effects in both the incident and exit channels. Finally, special efforts were made to extend the measurements of the angular distributions into $\theta_{Lab.}=4°$, thus sampling a region that is rarely, if ever, studied in such reactions, even though behavior at such forward angles should constitute a very important aspect of the overall problem of assessing how well we understand the basic nature of the reaction process.

III. ANALYSIS

The differential cross section for the two-nucleon pick-up reaction A(a,b)B can be expressed in the formalism of the distorted waves Born approximation (DWBA) as follows if spin-orbit coupling terms in the optical potentials of the entrance and exit channels are neglected:[19,20]

$$\frac{d\sigma}{d\Omega} = D_0^2 \sum_{LSJT} C_{ST}^2 \sum_{M} \left| \sum_{N} G_{NLSJT} B_{NL}^{M} \right|^2 . \qquad (1)$$

The term B_{NL}^{M} is the usual distorted-wave amplitude which

includes details of the interaction potential and the motion of the center of mass of the transferred pair. The factor G_{NLSJT} contains the nuclear structure information and is essentially determined by the wave functions of the initial and final nuclear states. The quantity D_0^2 is the normalization factor which arises in making the zero-range approximation. The coefficient C_{ST} is defined as

$$C_{ST} = (T_B N_B TN | T_A N_A) D(S,T) b_{ST} \qquad (2)$$

where the Clebsch-Gordon coefficient accounts for the coupling of the isospin of the residual nucleus, T_B, to that of the transferred pair, T, to yield the isospin of the target nucleus, T_A. The quantity b_{ST} is the spectroscopic factor for the light particles a and b, and has the values $b_{ST}^2 = 1/2$ for (p,^{3}He) reactions and unity for (p,t) reactions. The function D(S,T) depends on the strength of the spin-isospin exchange terms in the interaction potential and can be expressed as follows[1]

$$D(S,T) = 1-(0.5-\delta_{S,1})(B+H) \qquad (3)$$

The strength of the spin-isospin exchange force ($B+H=V_\sigma+V_\tau$) affects the relative values calculated for the (p,t) and (p,^{3}He) cross sections and, in addition, can affect the shapes of those (p,^{3}He) angular distributions in which more than one L value is allowed by the angular momentum selection rules. Actually, the quantity which is directly determined experimentally is the ratio of the triplet to singlet transfer strength

The details of the method of analysis used in the present work have been described previously.[19] DWBA calculations were carried out with the code DWUCK.[21] The form-factors were calculated separately and fed into DWUCK as data. The optical model parameters for the incident protons were adapted from Greenlees and Pyle.[18] The optical model potentials used for the outgoing tritons and ^{3}He particles (taken from Ref. 22) were identical to each other. This procedure is somewhat unusual, but the use of different optical parameters for the tritons and ^{3}He-particles prevents reliable results from being drawn from the comparison of (p,t) to (p,^{3}He) cross sections, since, as it was pointed out in a previous paper[13], the magnitudes of the calculated cross sections depend strongly on the depth of the absorbtive part of the mass-3 optical potential. In a recent paper[23] on the comparison of the inverse (^{3}He,p) and (t,p) reactions to isobaric analogue pairs of 0$^+$ states from ^{20}Ne to ^{56}Fe, Garrett and Hansen come to the same conclusion. The optical-model parameters we use in the present calculations are given in Table I. No radial cut-offs were employed.

The shell-model wave functions used in generating the form-factors are those of Wildenthal and McGrory.[24] The spectroscopic amplitudes for the various transitions analyzed in the present work are presented in Table II.

IV. RESULTS

A. Angular Distributions

The angular distributions obtained in the present measurements are displayed in Figs. 2-5. Error bars, where shown, reflect only statistical uncertainties. In the upper halves of Figs. 2 and 3 are displayed ^{29}Si(p,t)^{27}Si measurements, together with the results from DWBA calculations, while the ^{29}Si(p,^{3}He)^{27}Al measurements to the corresponding mirror levels, with DWBA calculations, are displayed in the lower halves of these figures. In the latter cases the contributions of the S=0,T=1 transfer (dotted curve) and the S=1, T=0 transfer (dashed-dotted curve) to the differential cross section (full curve) are shown separately. Figure 4 shows miscellaneous other (p,t) distributions, and Figure 5 displays the remaining (p,^{3}He) distributions.

The patterns of most of the (p,t) angular distributions are sufficiently characteristic of the L transfer involved to permit spectroscopic assignments. In some cases new spin assignments or confirmations of existing J$^\pi$ assignments can be made. The distributions to the 2.86, 3.80 and 5.08 MeV states in ^{27}Si show L=2 patterns which then imply positive parity and J=3/2 or 5/2. The state at 2.91 MeV in ^{27}Si was previously assigned as 9/2$^+$ or 5/2$^+$. The observed L=4 angular distribution eliminates the 5/2$^+$ value. The shape of the angular distribution for the transition to the 3.54 MeV state in ^{27}Si is characteristic of L=0, which yields the unique result

$J^{\pi}=1/2^{+}$. These assignments are consistent with the spins of the mirror levels in ^{27}Al.

In the ^{29}Si(p,^{3}He)^{27}Al reaction, more than one L value is allowed by the selection rules in many transitions. The resulting complexity caused us to refrain from drawing any new conclusions about possible spin values of states in ^{27}Al on the basis of the present data. In many instances, however, confirming evidence on spin-parity assignments based on other experimental techniques is obtained.

B. Transition Strengths

If, as is true in the present study for all (p,t) and some (p,^{3}He) transitions, only one L-value can contribute to a transition, the quantitative nuclear structure information available from the data is contained in the transition strength. The shapes in these cases are essentially independent of the details of the nuclear wave functions and are functions only of the L-transfer and of the general features of the DWBA analysis used. The strongest test of the wave functions in these instances is, therefore, their ability to predict the magnitudes of the cross sections. Ambiguities in the analysis of absolute cross-sections arise, however, both from experimental errors and from uncertainties in the overall normalization of zero-range DWBA calculations. Therefore only comparative studies of several transitions with identical experimental and analytical techniques are very meaningful in the present context.

For the purposes of evaluating how well the shell-model wave functions can account for the measured transition strengths we assume values of $D_0^2 = 20 \times 10^4$ MeV^{2}fm^3, $|D(0,1)|^2=0.72$, and $|D(1,0)|^2=0.30$ (R=0.42) in making the DWBA calculations. The value of D_0^2 is consistent with the overall normalizing factor found in other analyses of two-nucleon transfer data; the value of R, while qualitatively consistent with previous findings, is based on an analysis of the present data presented in Sec. V,A. The angular distributions calculated according to these procedures from the wave functions of Ref. 9. were then individually normalized to the experimental differential cross sections for the presumed corresponding transitions. The normalization factors σ_{exp}/σ_{th} thus extracted are presented in Table III. Good agreement between theory and experiment corresponds to a normalizing ratio of unity, and the over-all success of the shell model wave functions in dealing with these phenomena lies in the consistency with which this ratio remains close to unity for many states.

V. DISCUSSION

A. Spin-Isospin Dependence

The many approximations made in deriving the two-nucleon transfer differential cross section (Eq. 1) obscure the relationship of the spin-isospin dependence of the interaction potential used in calculating the transfer amplitudes to that of the nucleon-nucleon force. It is for this reason that an empirical unraveling of the effective value of the quantity from an analysis of

the data themselves is thought to be necessary. Unfortunately, as mentioned, an accurate determination of the strength of this spin-isospin dependent force is dependent upon the quality of the wave functions used to describe the initial and final states, i.e., upon the values of the spectroscopic amplitudes which weight each kind of transfer in each individual case. In order to elucidate the effects upon the determination of R (see Eq. 4) from comparative (p,t) and (p,^{3}He) studies which can result from different assumptions about the nuclear wave functions, three different sets of choices were made for the wave functions of the ground state of ^{29}Si and the first $1/2^+$, $3/2^+$, $5/2^+$ and $7/2^+$ states in ^{27}Al-^{27}Si.

In the lowest order shell model, the $1d_{5/2}$ shell is filled at ^{28}Si. The last neutron in ^{29}Si would then occupy the $2s_{1/2}$ shell, with the $1d_{3/2}$ shell being empty. The ground state of ^{27}Al-^{27}Si ($J^\pi=5/2^+$) is simply described as a hole in the $1d_{5/2}$ shell. In this picture excited states of ^{27}Al-^{27}Si can be obtained by removing a $1d_{5/2}$ nucleon into the $2s_{1/2}$ shell. The lowest $1/2^+$, $3/2^+$ and $7/2^+$ states are then characterized simply as $(1d_{5/2})^{10}_{0,1}\ (2s_{1/2})^1$, $(1d_{5/2})^{10}_{2,1}\ (2s_{1/2})^1$ and $(1d_{5/2})^{10}_{4,1}(2s_{1/2})^1$ configurations, respectively. The "complete" wave functions of Ref. 9 for these states have these configurations as the largest components. These one-component, or lowest shell-model wave functions are referred in the following as the ZOSM wave functions.

The second largest component predicted in the large shell-model calculations of Ref. 9 is in most cases a configuration which differs from the largest one only by removing a nucleon pair from an inner to an outer orbit. The second largest component of the ground-state wave function of ^{29}Si is of that type and is characterized as $(1d_{5/2})^{10}_{0,1}\ (2s_{1/2})^3$. But this type of configuration applied to ^{27}Al-^{27}Si cannot explain (nor can the ZOSM term) the experimentally observed large L=0 transfer component for the ^{29}Si(p,^{3}He) transition to the first $3/2^+$ state, for example. However, this restriction does not occur for a "1p-2h" configuration in which one particle is in the $2s_{1/2}$ shell and the two $1d_{5/2}$ holes are coupled to (J,T)=(1,0). Therefore such "recoupled" 1p-2h configurations are used as first-order corrections to the above ZOSM wave functions for the lowest $1/2^+$, $3/2^+$ and $7/2^+$ states of ^{27}Al-^{27}Si. As the second component of the ground state of ^{27}Al-^{27}Si the $(1d_{5/2})^{10}_{3,0}\ (2s_{1/2})^1$ configuration was chosen. The wave functions so constructed, consisting of only two components, are referred in the following as FOSM wave functions.

In the third approach the "complete" wave functions of Ref. 9 were used. These wave functions were calculated in a truncated $(1d_{5/2})^{n_1}\ (2s_{1/2})^{n_2}\ (1d_{3/2})^{n_3}$ vector space with $n_1\geq 8$ for ^{27}Al-^{27}Si, and with $n_1\geq 9$ plus $n_1=8$, $n_2=4$, $n_3=1$ for ^{29}Si. As the effective two-body interaction in those calculations the modified surface delta interation (MSDI) was used. In the following we refer to these as MSDI wave functions.

The influence of the strength of the spin-isospin interaction potential in the two-nucleon transfer amplitude was

studied by considering three different forces, a spin-isospin independent, or Wigner, force with B=H=0 (R=1.00, see Eq. 4), a Gillet force,[25] with B+H = 0.30, (R=0.42) and an empirically determined force[6] with B+H = 0.38, (R=0.28). These different spin-isospin dependent forces will not only produce different relative and absolute magnitudes of the overall (p,t) and (p,^{3}He) cross sections but will also produce different shapes of those (p,^{3}He) angular distributions which have multiple L-transfer components. We used these three choices of the ratio of the triplet to singlet transfer strength, R, together with the above described three sets of wave functions, and calculated the (p,t) and (p,^{3}He) differential cross sections for the transitions to the first four pairs of mirror states in ^{27}Si-^{27}Al, and compared the results to the experimental data. The shapes of the (p,t) angular distributions are unaffected by both the wave functions and the choice of R since the selection rules allow only pure L transfer, whereas in the (p,^{3}He) reaction, only the shape of the 1.01 MeV ($3/2^+$) angular distribution is markedly influenced by the different choices.

Figure 6 presents a comparison of the various theoretical angular distributions to the experimental data for the (p,t) transition to the 0.96 MeV state in ^{27}Si and for the (p,^{3}He) transition to the mirror 1.01 MeV state in ^{27}Al (denoted by A,B and C). For the (p,^{3}He) transition, three different comparisons were made. Part (A) shows the predictions of the three different sets of shell-model wave functions assuming a value of R=0.42. The ZOSM wave function allows only a $(1d_{5/2})^2_{2,1}$

transfer which leads to a pure L=2 angular distribution and does not fit the experimental data, which exhibits a large L=0 contribution. Besides this $(1d_{5/2})^2_{2,1}$ transfer, the FOSM wave functions allow also a $(1d_{5/2})^2_{1,0}$ transfer which does yield an L=0 contribution. This improves the fit but does not describe all the characteristics of the experimental angular distribution. The MSDI wave functions, finally, give a satisfactory account of the data, predicting quite well the envelope of the cross section.

Parts (B) and (C) of Figure 6 show the results obtained with the three different choices of R used in conjunction with the FOSM and MSDI wave functions, respectively. An increase of the strength of the spin-isospin interaction potential (lowering the value of R) enhances the S=0 transfer component relative to the S=1 component, which results in a decrease of the L=0 contribution. The FOSM wave functions fail to predict the shape of the experimental angular distribution even assuming a spin-isospin independent interaction potential (R=1.00). For the MSDI wave functions the value of R=0.42 gives the best agreement of the theoretical curve and the experimental data. It might seem that the curve with R=1.00 fits the experimental data better at very forward angles but the overall deviation from the data points is much larger than for the R=0.42 curve.

In Table IV are presented the experimental and theoretical cross section ratios obtained with the three different sets of

shell-model wave functions and the three different choices of R. These results, together with the study, discussed above, of the shape of the $(p,{}^3He)$ angular distribution to the 0.96 MeV level, were used as the basis for our choice of R=0.42 as the present working value for the spin-isospin dependence strength. Both on the basis of the shape of the $3/2^+(p,{}^3He)$ distribution and on an inspection of the scatter about unity of the values in Table IV for the various values of R, as well as upon general principles, we think that of the three sets tried, the full MSDI wave functions most nearly simulate reality. Hence we restricted our attention in determining R to the MSDI results. The choice then devolves into selecting which set of numbers in the last two columns of Table IV is more consistent with unity. The value R=0.42 seems to satisfy this requirement best, but the large scatter and the relatively small number of samples make a quantitative assessment of the uncertainty in this choice very difficult.

It seems fairly obvious that a study on a finer grid of values of R would not be meaningful. Also, it cannot be claimed that the present results by themselves rule out R=1.0 or some value even smaller than 0.28. All other aspects being favorable, however, we think that two or three more such studies should yield a value good to about 20% with a 50% confidence level.

B. Transitions to the Individual Mirror Levels

In the following discussion of the transitions to the individual mirror levels, the "MSDI" wave functions were used in the DWBA calculations and the values $|D(S=0)|^2 = 0.72$ and $|D(S=1)|^2 = 0.30$ for the singlet and triplet transfer strengths, respectively, were assumed. The normalizing factors of Table III are used as the basis of comments about the strengths of the transitions.

1. Ground State (^{27}Si and ^{27}Al), $J^\pi=5/2^+$.

The strengths of the ground-state transitions are about one order of magnitude larger than of the other transitions. The shell-model wave functions predict a predominant $(1d_{5/2})$, $2s_{1/2})_{2,1}$ transfer, with some $(1d_{5/2})^2_{3,0}$ admixture in the $(p,{}^3He)$ case. A quite good account of the shape of the (p,t) and $(p,{}^3He)$ angular distribution is obtained (see Fig. 2), although the minimum around 35° in the (pkt) data is not reproduced. The magnitude of the (p,t) cross section is overestimated by nearly a factor of two. If one neglects the T=0 contribution in the $(p,{}^3He)$ cross section one obtains the ratio $\sigma_{exp}/\sigma_{th} = 1.27$, which is equal to that found for the (p,t) transition. In a previous study[15] of the inverse reaction, $^{27}Al(^3He,p)^{29}Si$, a significant L=4 contribution, in addition to the dominant L=2 component, was experimentally

found for this transition. The present data do not show strong evidence for an L=4 component.

2. E_x=0.78(^{27}Si) and 0.84(^{27}Al) MeV, $J^\pi = 1/2^+$.

The experimental angular distributions exhibit the characteristic pattern of L=0 transfer (see Fig. 2), and their shapes are well reproduced by the calculation. The shell-model wave functions slightly overpredict the T=1 transfer component, as can be seen from the (p,t) cross section ratio $\sigma_{exp}/\sigma_{th} = 0.75$. A slight reduction of this T=1 transfer component gives a better agreement in the (p,t) case but has nearly no influence on the good agreement predicted for the (p,^{3}He) cross section since this is predominantly determined by the T=0 transfer component.

3. E_x=0.96(^{27}Si) and 1.01(^{27}Al) MeV, $J^\pi = 3/2^+$.

These transitions were discussed extensively in the previous section which concerned the strength of the spin-isospin dependent interaction potential.

4. E_x=2.16(^{27}Si) and 2.21(^{27}Al) MeV, $J^\pi = 7/2^+$.

The selection rules allow only an L=4 transfer in the (p,t) reaction, whereas in the (p,^{3}He) reaction both L=2 and L=4 are possible. The experimental angular distributions are quite nicely reproduced by the shell-model wave functions (see Fig. 2), although the magnitude of the (p,t) cross section is overestimated by nearly a factor of two.

5. E_x=2.65(^{27}Si) and 2.73(^{27}Al) MeV, $J^\pi = 5/2^+$.

Both the (p,t) and the (p,^{3}He) angular distributions (see Fig. 2) exhibit an L=2 pattern, but the (p,t) data points drop down at very forward angles, a behavior contrary to the usual L=2 pattern shown in other transitions. Besides failing to account for this anomaly, the fit to the (p,t) data is of poor quality in general. Beyond that, the magnitude of the cross section is underpredicted by a factor of four. The shell-model wave functions reproduce the shapes of the (p,^{3}He) angular distribution quite well and overestimate the magnitude somewhat.

6. E_x=3.54(^{27}Si) and 3.68(^{27}Al) MeV, $J^\pi = 1/2^+$.

The selection rules restrict the (p,t) transition to be pure L=0 while the (p,^{3}He) can be a mixture of L=0 and L=2. The shapes of both the (p,t) and (p,^{3}He) angular distributions are well reproduced by the DWBA calculations (see Fig. 3). The magnitude of the (p,t) cross section is well predicted whereas it is overpredicted for the mirror (p,^{3}He) transition by nearly a factor of two. The main contribution of the (p,^{3}He) cross section comes from the T=0 transfer, which is forbidden in the (p,t) reaction. A reduction of this T=0 transfer contribution would accordingly bring about a better agreement between the theory and the experimental data.

7. E_x=3.80(^{27}Si) and 3.96(^{27}Al) MeV, $J^\pi = 3/2^+$.

For the (p,t) transition the selection rules allow only an L=2 transition while for the (p,^{3}He) transition a mixture of L=0 and L=2 is allowed. The shell-model wave functions give

a very good account of the shape and the magnitude of the (p,t) angular distribution (see Fig. 3) but, for the (p,^{3}He) angular distribution, the predicted L=0 contribution is too large. The experimental data can be fitted by a pure L=2 angular distribution. The magnitude of the (p,^{3}He) transition strength is overestimated by nearly a factor of three. A drastic reduction of the T=0 component, which is responsible for the L=0 transfer contribution, improves the agreement between the theoretical curve and the experimental data with respect to both the magnitude and the angular dependence of the differential cross section.

8. E_x=4.29(^{27}Si) and 4.41(^{27}Al) MeV, $J^\pi = 5/2^+$.

The (p,t) transition can proceed only by a pure L=2 transfer and the (p,^{3}He) transition by both L=2 and L=4. The DWBA calculations predict the shape and the magnitude of the (p,t) differential cross section quite well (see Fig. 3). The shape of the (p,^{3}He) angular distribution is reasonably well reproduced, although the data show the same strange behavior at small angles as did the (p,t) angular distribution of the 2.65 MeV transition. The magnitude of the (p,^{3}He) transition strength is overestimated by a factor of three. Here again the shell-model wave functions give a very good account of the T=1 transfer contribution but fail to predict the T=0 part.

9. E_x=2.86,2.91(^{27}Si) and 2.98,3.00(^{27}Al) MeV, $J^\pi = 3/2^+, 9/2^+$.

Since in the (p,^{3}He) reaction, the transitions to these two states could not be experimentally resolved, the transitions to the two mirror states are also analyzed together (the separated

(p,t) angular distributions are shown in Fig. 4). Both the experimental (p,t) and (p,^{3}He) angular distributions show the L=4 patterns which are only allowed for the transitions to the $9/2^+$ states. Thus the contributions from the transitions to the $3/2^+$ states are very weak. For the transition to these $3/2^+$ states the shell model wave functions predict a very weak T=1 transfer component, as can be seen from the (by a factor of 98) underestimated magnitude of the (p,t) transiction strength, and a large T=0 transfer component which yields a pure L=0 pattern for the (p,^{3}He) angular distribution which does not fit the experimental data. Thus the wave functions fail completely to describe the observed two-nucleon pick-up features to these $3/2^+$ states in ^{27}Si-^{27}Al. The shape of the (p,t) cross section to the $9/2^+$ state is well predicted whereas its magnitude is underestimated by a factor of 15. The (p,^{3}He) data are quite nicely fitted by the transition to the $9/2^+$ state alone with respect to both the shape and the magnitude of the differential cross section.

C. Comments on the Observed Shapes of the Angular Distributions

As already mentioned in the discussion of the transitions to the individual mirror levels, there are discrepancies in some angular distributions between the experimental data and the theoretical predictions which cannot be connected with inadequacies in the shell-model wave functions. This is particularly surprising in the light of the success we have had in reproducing

REFERENCES

1. J. C. Hardy, and I. S. Towner, Phys. Lett. 25B,98(1967).
2. D. G. Fleming, J. Cerny, and N. K. Glendenning, Phys. Rev. 165,1153(1968).
3. D. G. Fleming, J. Cerny, C. C. Maples, and N. K. Glendenning, Phys. Rev. 166,1012(1968).
4. J. C. Hardy, H. Brunnader, and J. Cerny, Phys. Rev. Lett. 22,1439(1969).
5. J. C. Hardy, A. D. Bacher, G. R. Plottner, J. A. Macdonald, and R. G. Sextro, Phys. Rev. Lett. 25,298(1970).
6. D. G. Fleming, J. C. Hardy, and J. Cerny, Nucl. Phys. A162,225(1971).
7. B. Vignon, J. F. Bruandet, N. Longequeue, and I. S. Towner, Nucl. Phys. A162,82(1971).
8. J. M. Nelson, and W. R. Falk, Nucl. Phys. A218,441(1974).
9. B. H. Wildenthal and J. B. McGrory, Phys. Rev. C7,714 (1973).
10. B. H. Wildenthal, J. B. McGrory, E. C. Halbert and H. D. Graber, Phys. Rev. C4,1708(1971).
11. B. H. Wildenthal, E. C. Halbert, J. B. McGrory, and T.T.S. Kuo, Phys. Rev. C4,1266(1971).
12. B. M. Preedom and B. H. Wildenthal, Phys. Rev. C6,1633 (1972).
13. H. Nann, B. Hubert, and R. Bass, Nucl. Phys. A176,553 (1971).

14. B. Hubert, H. Nann, W. Schäfer, and R. Bass, Nucl. Phys. A192,1(1972).
15. H. Nann, L. Armbruster, and B. H. Wildenthal, Nucl. Phys. A198,11(1972).
16. H. Nann, B. H. Wildenthal, H. H. Duhm, and H. Hafner, to be published.
17. W. A. Lanford, et al., Bull. Am. Phys. Soc. 17,895(1972).
18. G. W. Greenlees, and G. J. Pyle, Phys. Rev. 149,836(1966) and F. D. Bechetti and G. W. Greenlees, Phys. Rev. 182,1190(1969).
19. N. K. Glendenning, Phys. Rev. 137,B102(1965).
20. I. S. Towner and J. C. Hardy, Adv. in Phys. 18,401(1969).
21. P. D. Kunz, University of Colorado, private communication.
22. H. P. Morsch, and R. Santo, Nucl. Phys. 179,401(1972).
23. J. D. Garrett, and O. Hansen, Nucl. Phys. A212,600(1973).
24. P. M. Endt, and C. van der Leun, Nucl. Phys. A214,1(1973).
25. V. Gillet, and N. Vinh-Mau, Nucl. Phys. 54,321(1964).
26. G. R. Satchler, Proc. Int. Conf. on Nuclear Physics, Munich 1973, Vol. 2, p. 569.

TABLE I.--Optical-model parameters used in the DWBA calculations.

	V (MeV)	W (MeV)	W' (MeV)	r_o (fm)	a (fm)	r_c (fm)	r_o' (rm)	a' (fm)
p	45.5		13.0	1.20	0.70	1.25	1.25	0.70
^{3}He,t	173.9	20.6		1.15	0.72	1.40	1.50	0.82

TABLE II.--Spectroscopic amplitudes for ^{29}Si→A=27.

J_B	T_B	E_x (MeV)	J	T	(D5,D5)	(S1,S1)	(D3,D3)	(D5,S1)	(D5,D3)	(S1,D3)
$1/2^+$	1/2	0.50	0	1	-.783	.201	-.069			
			1	0	-.186	.425	-.026		-.087	-.008
		2.85	0	1	.200	.180	.030			
			1	0	-.671	-.072	.075		-.030	-.065
		5.35	0	1	.060	.208	.030			
			1	0	-.108	.151	-.006		-.112	-.002
$3/2^+$	1/2	1.02	1	0	-.486	-.088	.027		.161	-.056
			2	1	-1.070		-.003	.084	-.344	.086
			2	0				.111	.157	.045
		2.78	1	0	-.626	-.137	.024		.032	.110
			2	1	.128		.018	-.188	-.140	.194
			2	0				-.161	-.002	.136
		3.81	1	0	-.608	-.137	.058		-.051	-.179
			2	1	.307		.043	.349	.062	-.012
			2	0				.254	-.087	-.063
$5/2^+$	1/2	0.00	2	1	.400		.146	1.393	-.085	.324
			2	0				-.753	.033	-.179
			3	0	.355		-.036	.748	.080	
		3.07	2	1	.621		-.084	-.492	-.327	.082
			2	0				.248	.126	-.043
			3	0	.828		.014	-.516	.077	
		3.98	2	1	.801			-.157	-.033	.107
			2	0				.076	.046	-.057
			3	0	-.553		.016	-.440	.006	
		4.59	2	1	-.530		-.031	-.124	.024	-.046
			2	0				-.148	-.015	-.012
			3	0	-.105		.006	-.342	-.036	
$7/2^+$	1/2	1.84	3	0	.460		.003	.058	-.283	
			4	1	1.648				.201	
			4	0	.000				-.160	
		4.52	3	0	.977		-.051	.138	-.020	
			4	1	-.021				.013	
			4	0					-.047	
$9/2^+$	1/2	2.76	4	1	-.730				.469	
			4	0					-.239	
			5	0	-1.552					
$11/2^+$	1/2	3.91	5	0	1.532					
		5.25	5	0	.840					

TABLE IV.--Comparison of experimental and theoretical cross sections for three different sets of shell-model wave functions and different choices of R.

J	$E_x(^{27}Al)$ (MeV)	$E_x(^{27}Si)$ (MeV)	R	σ_{exp}/σ_{th} ZOSM $(p,^3He)$	ZOSM (p,t)	FOSM $(p,^3He)$	FOSM (p,t)	MSDI $(p,^3He)$	MSDI (p,t)
$5/2^+$	0.00	0.00	1.00	0.14	0.90	0.17	2.25	0.25	0.90
			0.42	0.36	1.25	0.45	3.10	0.58	1.25
			0.28	0.50	1.40	0.68	3.50	0.79	1.40
$1/2^+$	0.84	0.78	1.00	0.80	0.14	0.26	0.55	0.40	0.54
			0.42	1.10	0.19	0.80	0.75	1.05	0.75
			0.28	1.23	0.21	1.20	0.85	1.80	0.84
$3/2^+$	1.01	0.96	1.00	1.51	0.27	1.08	0.47	0.47	0.54
			0.42	2.10	0.38	2.10	0.65	1.30	0.75
			0.28	2.35	0.42	2.80	0.73	2.25	0.84
$7/2^+$	2.21	2.16	1.00	1.08	0.34	0.80	0.50	0.40	0.43
			0.42	1.50	0.48	1.50	0.70	0.90	0.60
			0.28	1.68	0.53	1.85	0.80	1.13	0.67

TABLE III:--Comparison of experimental and theoretical cross sections to states in ^{27}Al-^{27}Si.

J^π	E_x(theor.) (MeV)	$E_x(^{27}Al)$ (MeV)	$E_x(^{27}Si)$ (MeV)	σ_{exp}/σ_{th} $(p,^3He)$	(p,t)
$5/2^+$	0.00	0.00	0.00	0.58	1.25
$1/2^+$	0.50	0.84	0.78	1.05	0.75
$3/2^+$	1.02	1.01	0.96	1.30	0.75
$7/2^+$	1.84	2.21	2.16	0.90	0.60
$5/2^+$	3.07	2.73	2.65	0.65	4.10
$3/2^+$	2.78	2.98	2.86	0.75	20.0 98.0 15.0
$9/2^+$	2.76	3.00	2.91		
$1/2^+$	2.85	3.68	3.54	0.60	1.20
$3/2^+$	3.81	3.96	3.80	0.35	0.95
$5/2^+$	3.98	4.41	4.29	0.28	0.90
$11/2^+$	3.91	4.51		0.55	
$7/2^+$	4.52	4.58			
$5/2^+$	4.59	4.81	4.72		2.30
$1/2^+$	5.35	5.75		2.50	

FIGURE CAPTIONS

Fig. 1.--Energy spectra for the reactions $^{29}Si(p,t)^{27}Si$ and $^{29}Si(p,^{3}He)^{27}Al$ at 8°.

Fig. 2.--Angular distributions for transitions to mirrors final states in ^{27}Si and ^{27}Al populated in the $^{29}Si(p,t)$--upper half--and $^{29}Si(p,^{3}He)$--lower half--reactions, respectively. The curves represent DWBA calculations.

Fig. 3.--Angular distributions for the reactions $^{29}Si(p,t)^{27}Si$ (upper half) and $^{29}Si(p,t)^{27}Al$ (lower half) leading to mirror states. The curves represent DWBA calculations.

Fig. 4.--Triton angular distributions for miscellaneous levels in ^{27}Si. The curves are DWBA fits to the data.

Fig. 5.--^{3}He angular distributions for miscellaneous levels in ^{27}Al. The curves are DWBA fits to the data.

Fig. 6.--Comparison of various theoretical angular distributions to the experimental data for the (p,t) transition to the 0.96 MeV state in ^{27}Si and for the $(p,^{3}He)$ transition to the mirror 1.01 MeV state in ^{27}Al (denoted by A,B and C). For further explanations see text.

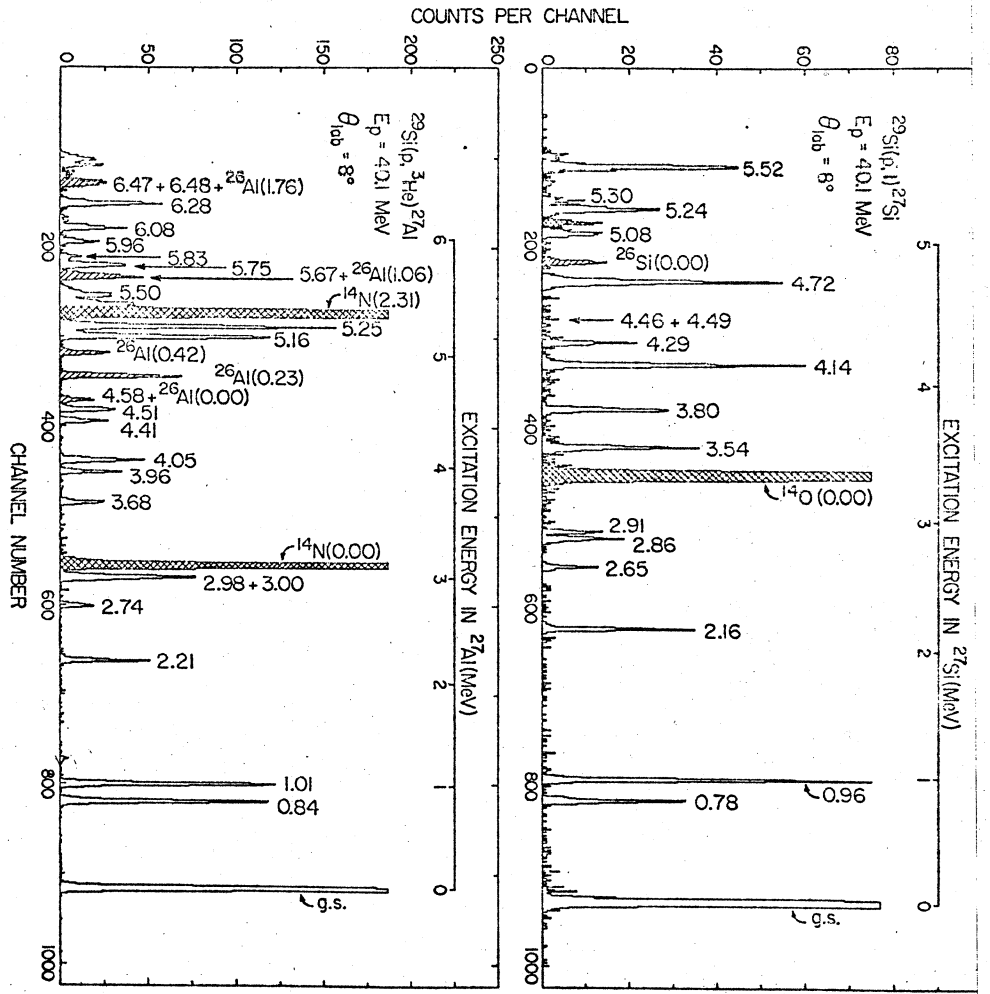

Figure 1

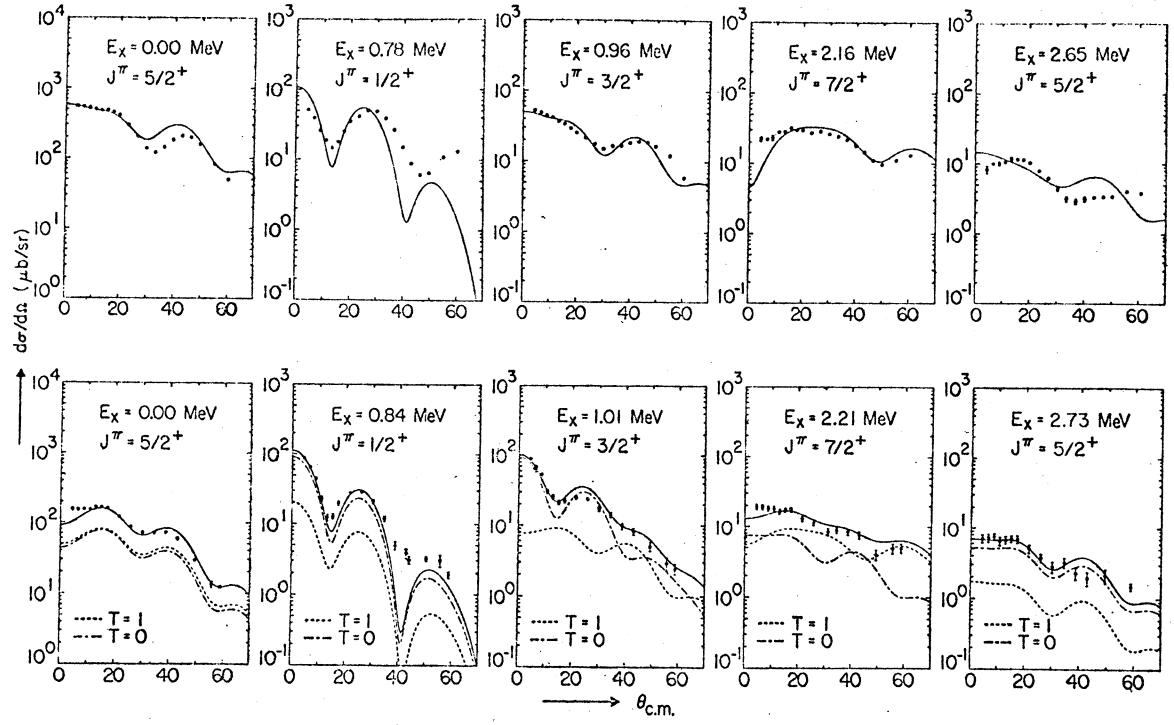

Figure 2

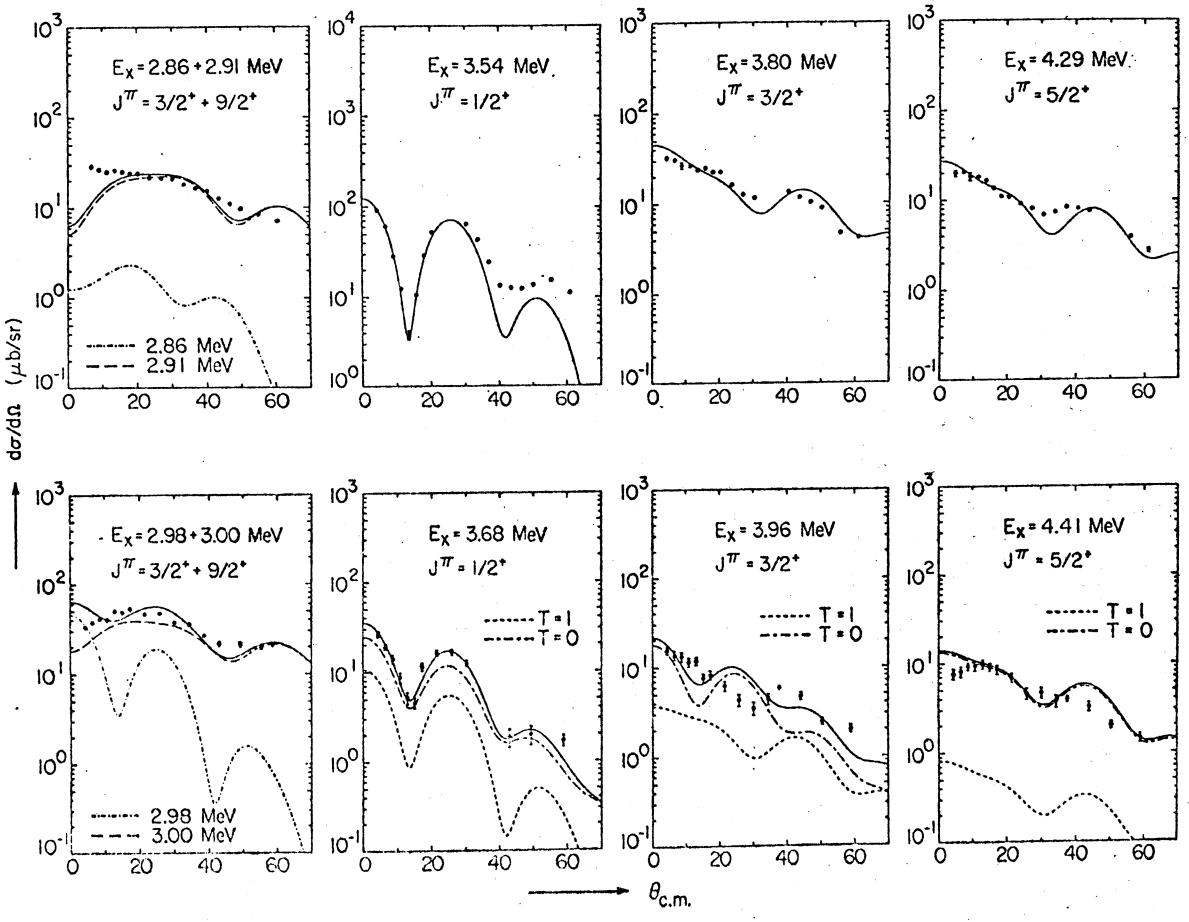

Figure 3

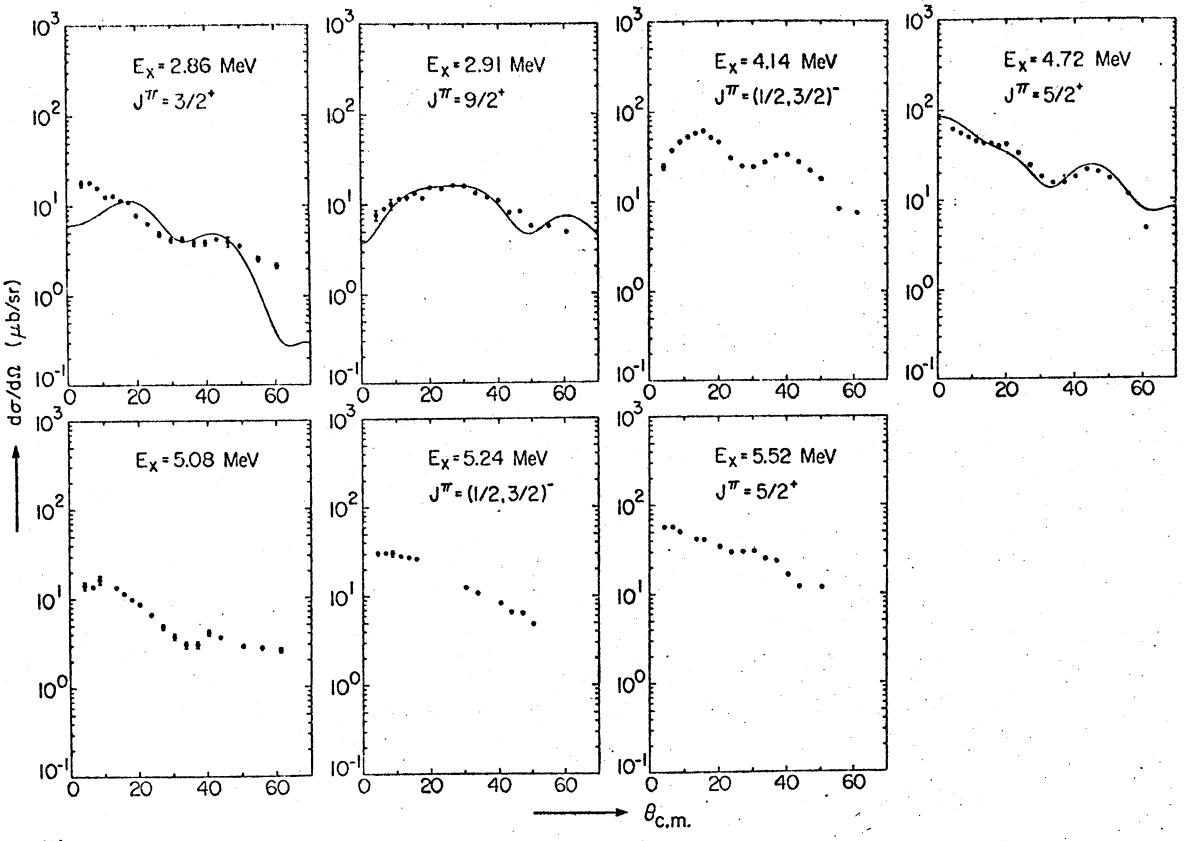

Figure 4

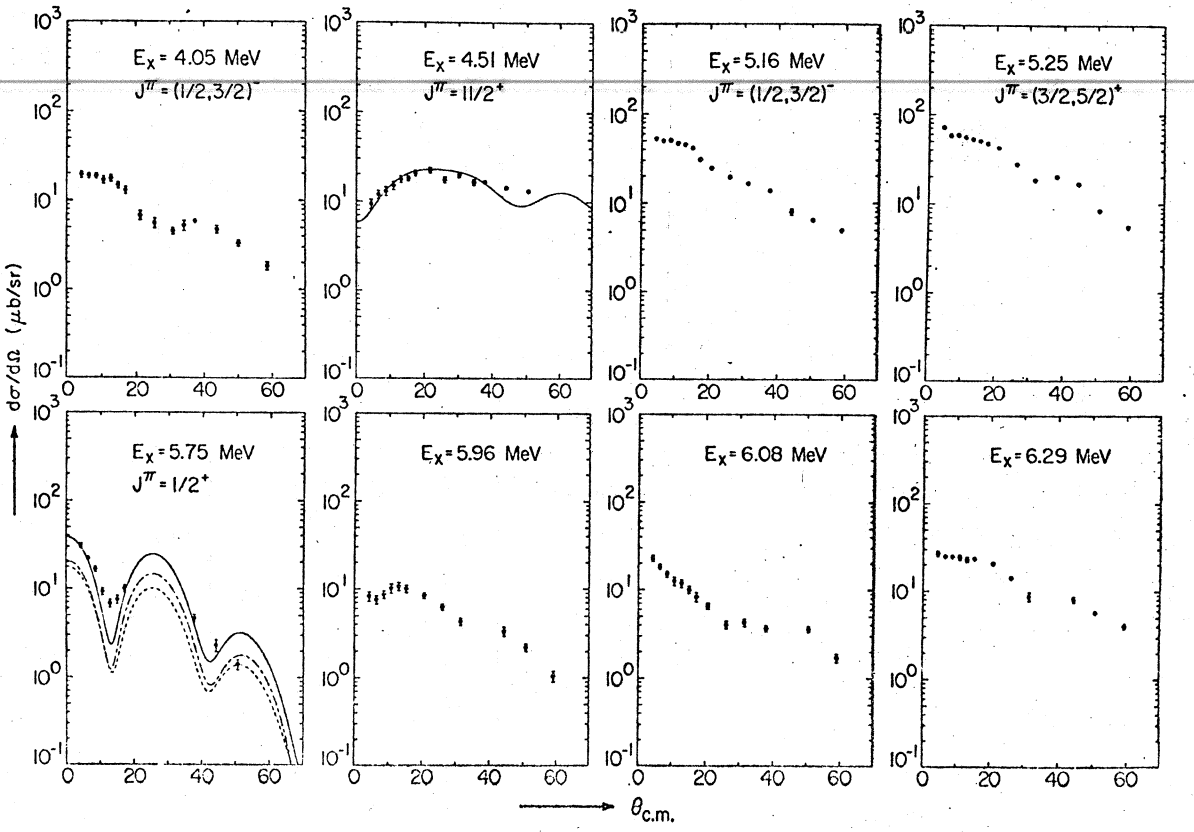

Figure 5

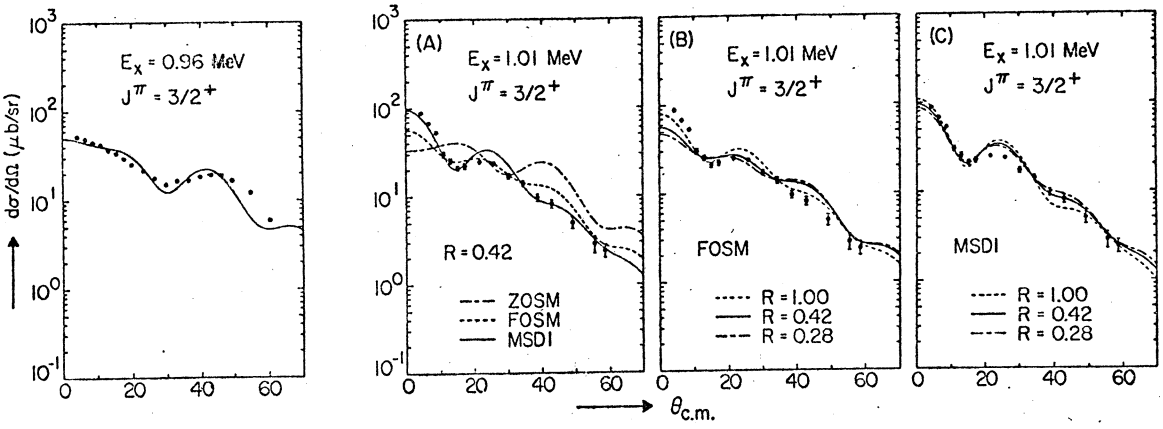
E_x = 0.96 MeV
$J^\pi = 3/2^+$
$d\sigma/d\Omega$ (μb/sr)
(A)
E_x = 1.01 MeV
$J^\pi = 3/2^+$
R = 0.42
ZOSM
FOSM
MSDI
(B)
E_x = 1.01 MeV
$J^\pi = 3/2^+$
FOSM
R = 1.00
R = 0.42
R = 0.28
(C)
E_x = 1.01 MeV
$J^\pi = 3/2^+$
MSDI
R = 1.00
R = 0.42
R = 0.28
$\theta_{c.m.}$

Figure 6